Current distribution in B- and N-doped carbon nanotubes

Yi Liu and Hong Guo
Center for the Physics of Materials and Department of Physics, McGill University, Montreal, PQ, Canada H3A 2T8
(Received 29 May 2003; revised manuscript received 29 September 2003; published 4 March 2004)

Using density functional theory and Keldysh nonequilibrium Green's functions, we investigate electron current density distribution in molecular electronic devices. In particular, we present the current distribution in pristine (5,5) armchair carbon nanotube as well as in nanotubes with substitutional doping of boron and nitrogen impurity atoms. The presence of impurity breaks the uniformity of current distribution around the carbon rings. For the more electronegative impurity of nitrogen, the current density is attracted toward the side of the tube where the N atom is located; but for the less electronegative impurity of boron, the opposite happens. Accordingly there appears a chiral flow of current in the B- and N-doped armchair nanotube near the impurity.

DOI: 10.1103/PhysRevB.69.115401 PACS number(s): 81.07.De, 72.80.Rj, 85.65.+h, 73.23.Ad

In recent years, there is a rapid development in fabricating and investigating molecular electronic devices[1] based on single molecule[2–5] or molecular strands.[6–8] Such a device is typically connected to a circuit by two or more leads where bias voltage is applied and current is collected. Many theoretical analysis have been devoted to the understanding of the basic physics of these systems.[9–13] A particularly important question is concerning how electric current flows through a molecule. This question has so far been investigated mainly through the alignment of molecular levels to the Fermi levels of the leads,[14] the nature of the molecular levels which mediate transport,[15] and the role played by the molecular-lead contacts. These investigations have provided useful understanding and insight on the property of *total* electric current that is flowing through a device.

In this work, we investigate current flow from a different perspective, namely from the point of view of current density distribution. Current density gives *local* information of nonequilibrium transport, thereby providing useful and vivid insight to transport properties of molecular electronics. At the molecular scale, current density is expected to be nonuniform, but how nonuniform is it? For molecules doped with impurity atoms, how does the current density change? Due to atomic bonding structure, chiral current may occur as theoretically demonstrated in BC_2N nanotube[16] and C_{60} molecules.[17] Can chiral current occur in impurity doped nanotubes? These are interesting questions because a nonuniform current density may provide a local heating that is different from the average behavior. To the best of our knowledge, there has been one discussion on current density distribution at molecular scale for a C_{60} tunnel junction[17] where very interesting results were obtained on local current loops along the carbon bonds. In this paper we further examine issues related to current-density distribution. In particular, instead of using tight binding models at equilibrium,[17] our analysis is based on an *ab initio* formalism which combines the density functional theory (DFT) with the Keldysh nonequilibrium Green's functions (NEGF).[12,13]

In the following we focus on two-probe devices in the form of electrode-molecule-electrode. Here an electrode has its own atomic structure with a translational symmetry, while the molecule refers to a molecular scale scattering region involving many atoms. We apply our NEGF-DFT formalism[12] to investigate current density distribution in armchair carbon nanotubes with boron or nitrogen substitutional doping. It was pointed out before[16] that carbon nanotubes cannot have a chiral current, because the graphitic tubule walls have isotropic in-plane conductivity which inhibits chiral current. However, when carbon nanotubes are doped by foreign impurities, the situation is different. Because the current density in doped nanotubes is substantially influenced by the impurity, there appears anisotropic electron current. Our results show that for the more electronegative impurity of N, current density is found to be largely ''attracted'' toward the side of the tube where the N atom is located (except in the very close vicinity of the N atom); for the less electronegative impurity of B, current density is largely ''repelled'' to the other side of the tube where there is no B doping (except in the very close vicinity of the B atom). From the current density distribution, we deduce that there is chiral current flow in the B- and N-doped armchair carbon nanotubes near the impurity.

The NEGF-DFT technique which we use has been discussed previously and we refer interested readers to the original paper.[12] Very briefly, our analysis uses an s, p, d real space LCAO basis set[12,18] and the atomic cores are defined by the standard nonlocal norm conserving pseudopotential.[19] The density matrix of the device is constructed via NEGF and the external bias V_b provides the electrostatic boundary conditions for the Hartree potential which is solved in a three dimensional real space grid. Once the density matrix is obtained, the Kohn-Sham effective potential $V_{\rm eff}(\mathbf{r};V_b)$, which includes contributions from Hartree, exchange, correlation, and the atomic core, is calculated. This process is iterated until numerical convergence of the self-consistent density matrix is achieved. In this way, we obtain the bias dependent self-consistent effective potential $V_{\rm eff}(\mathbf{r};V_b)$, from which we calculate[12] the transmission coefficient $T(E,V_b)\equiv T(E,[V_{\rm eff}(\mathbf{r},V_b)])$, where E is the scattering electron energy and T is a function of bias V_b through its functional dependence on $V_{\rm eff}(\mathbf{r};V_b)$. The NEGF-DFT technique has several characteristics very useful for our purpose.[12,13] (i) The formalism constructs charge density under external bias potential using NEGF, thereby treats open

device structures within the full self-consistent atomistic model of DFT. (ii) It treats atoms in the device and the leads at equal footing so that realistic atomistic leads is used. (iii) It treats localized and scattering states at equal footing so that the charge density includes all of these contributions. (iv) It is numerically efficient so that rather large systems can be analyzed.

After the device Hamiltonian $\hat{H}$ [i.e., the effective potential $V_{\text{eff}}(\mathbf{r};V_b)$] is self-consistently calculated within the NEGF-DFT formalism, we proceed to calculate current density. The electron current density is obtained from the scattering states of the device

$$\mathbf{J}=\sum_i \mathbf{J}_i, \tag{1}$$

where

$$\mathbf{J}_i=-\frac{i\hbar}{2m}[\Psi_i^*\nabla\Psi_i-\Psi_i\nabla\Psi_i^*]. \tag{2}$$

Here Ψ_i is the ith scattering state which is defined in the energy range $\mu_{\min}<E<\mu_{\max}$, where $\mu_{\min}/\mu_{\max}$ is the minimum/maximum of the electrochemical potentials of the left/right leads μ_L,μ_R, and $|\mu_R-\mu_L|=eV_b$, where V_b is the external bias voltage.

To solve the scattering states at a given energy E, $\Psi_i=\Psi_i(E)$, we proceed as follows.[12] Inside an electrode, $\Psi_i(E)$ can be expressed as a linear combination of the Bloch states. These Bloch states at a given E can be obtained by solving an inverse energy band structure problem.[12] Inside the scattering region, Ψ_i is represented as a linear combination of atomic orbitals. We then group all states as left and right propagating states depending on their group velocity. For a scattering state coming from the left electrode, $\Psi^{K_n^L}$ should start as a right propagating state $\Phi_L^{K_n^L}$ and it reflect back as a left propagating state $\phi_L^{K_m^L}$ with reflection coefficient $r^{K_m^L,K_n^L}$ in the left electrode, and transmit into the right electrode as a right propagating state $\phi_R^{K_m^R}$ with transmission coefficient $t_R^{K_m^R,K_n^L}$. Therefore, for example, a left scattering state can be written as

$$\Psi^{K_n^L}=\begin{cases}\Phi_L^{K_n^L}+\phi_L^{K_m^L}r^{K_m^L,K_n^L} & \text{in the left electrode,}\\ \psi_d^{K_n^L} & \text{in the scattering region,}\\ \phi_R^{K_m^R}t^{K_m^R,K_n^L} & \text{in the right electrode.}\end{cases}$$

A scattering state in the right electrode can be written in a similar way. For a symmetric two probe device, the total transmission from the left electrode is identical to the one from the right electrode. The matrix equation obtained by applying the device Hamiltonian $\hat{H}$ to the scattering states can be solved to obtain the transmission and reflection coefficients, as well as the scattering states inside the scattering region. Finally, we calculate current density from Eq. (2) by a finite differencing numerical technique.

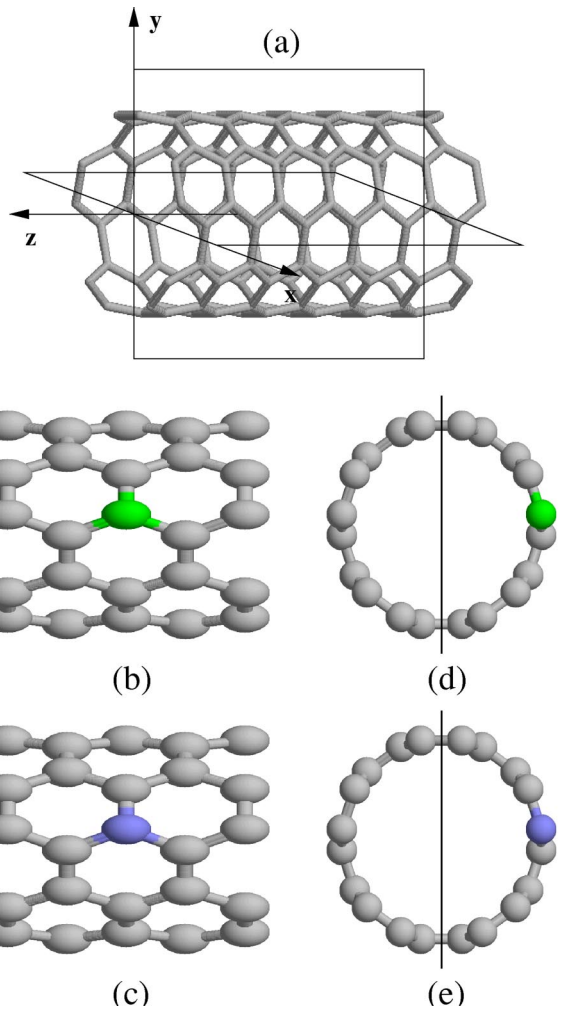

FIG. 1. (Color online) (a) Schematic illustration of the coordinates we use on the pristine and B- and N-doped (5,5) nanotubes. (b) and (d) The profile and cross section of the boron-doped (5,5) nanotube. (c) and (e) The profile and cross section of the nitrogen-doped (5,5) nanotube.

In the following we investigate current density distribution of B- and N-doped carbon nanotubes. A perfect single-wall carbon nanotube (SWNT) is either metallic or semiconducting depending on its chirality and diameter, which are determined by the chiral vector (n,m).[20–22] Both experimental[23–26] and theoretical[27–31] studies have shown that electronic and transport properties of a SWNT can be substantially modified by defects such as topological imperfections, vacancies, impurities, and deformations. For metallic nanotubes such as the armchair (5,5) tube, substitutional B and N impurity is expected to reduce the overall conductance because it provides a backscattering center, as demonstrated already in Ref. 30. For the metallic nanotube, the current voltage characteristic is linear as reported before.[32] In the following we present impurity effects on current density distribution on (5,5) tubes with a single B or N substitution. In our analysis, we have neglected the very small lattice distortion due to substitution.[33] Since current density is a vector field, we plot it in the x-z and y-z planes shown in Fig. 1(a). In particular, the x-z plane cuts through the doped

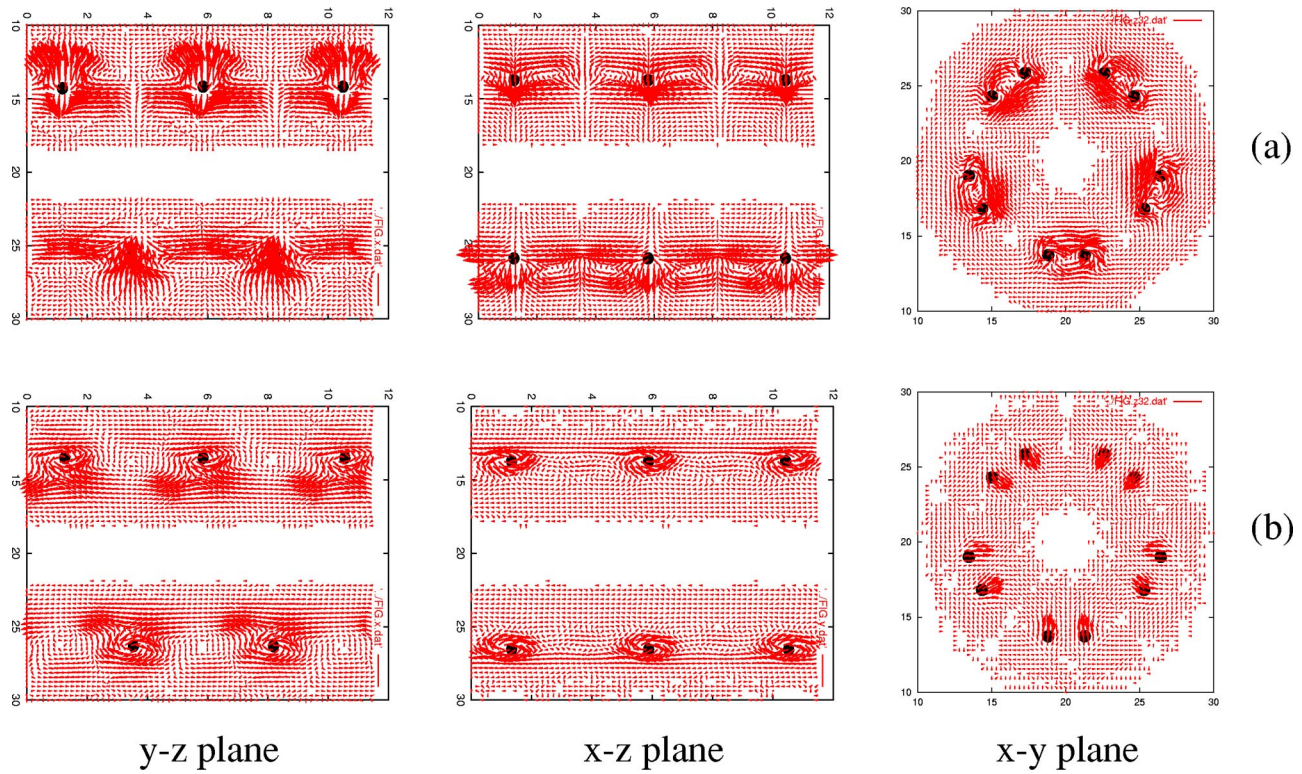

FIG. 2. (Color online) Distribution of the current density in the pristine (5,5) nanotube. The length of the arrows is proportional to the value of local current density. (a) The projections of the current density onto corresponding planes at zero bias voltage $V_b=0$. (b) At $V_b=0.8$ V.

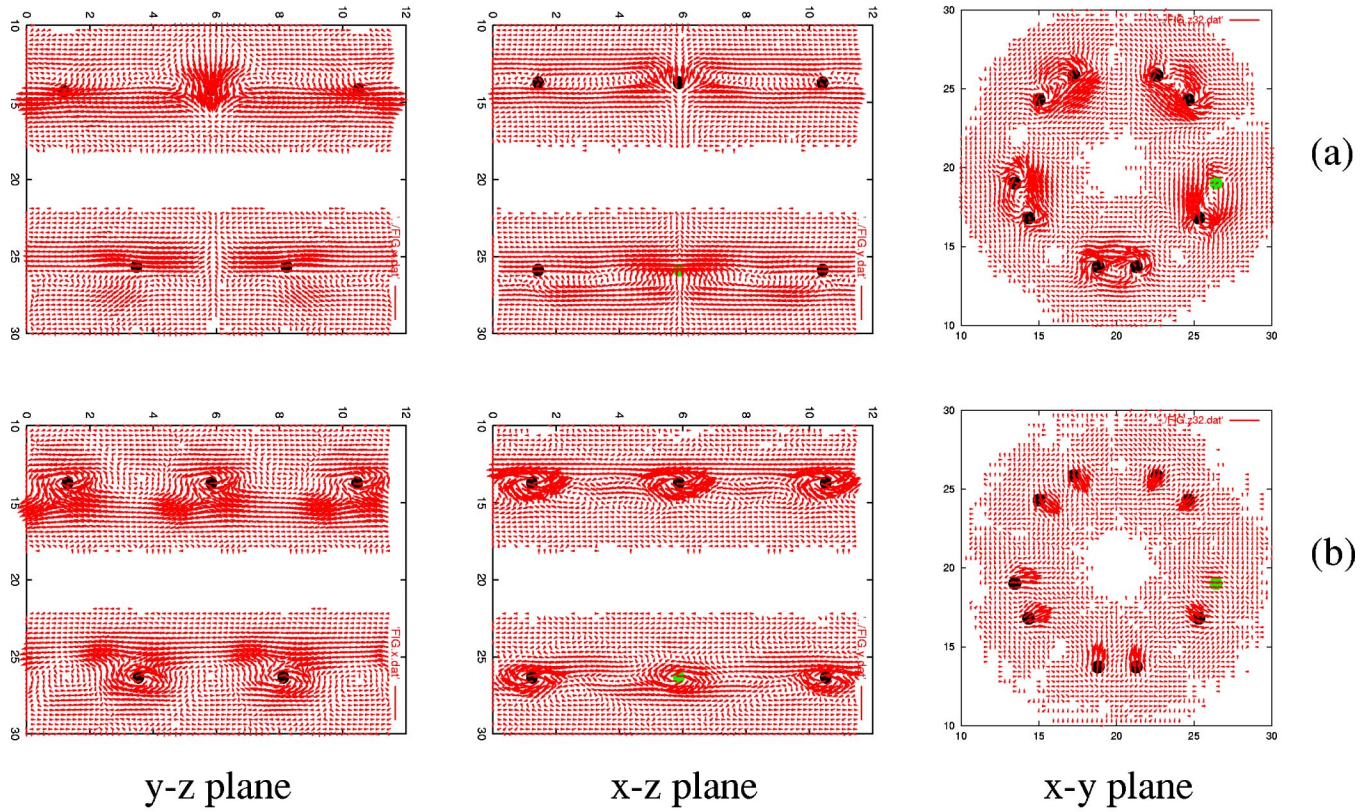

FIG. 3. (Color online) Distribution of the current density in the boron-doped (5,5) nanotube. (a) The projections of current density at $V_b=0$, (b) at $V_b=0.8$ V.

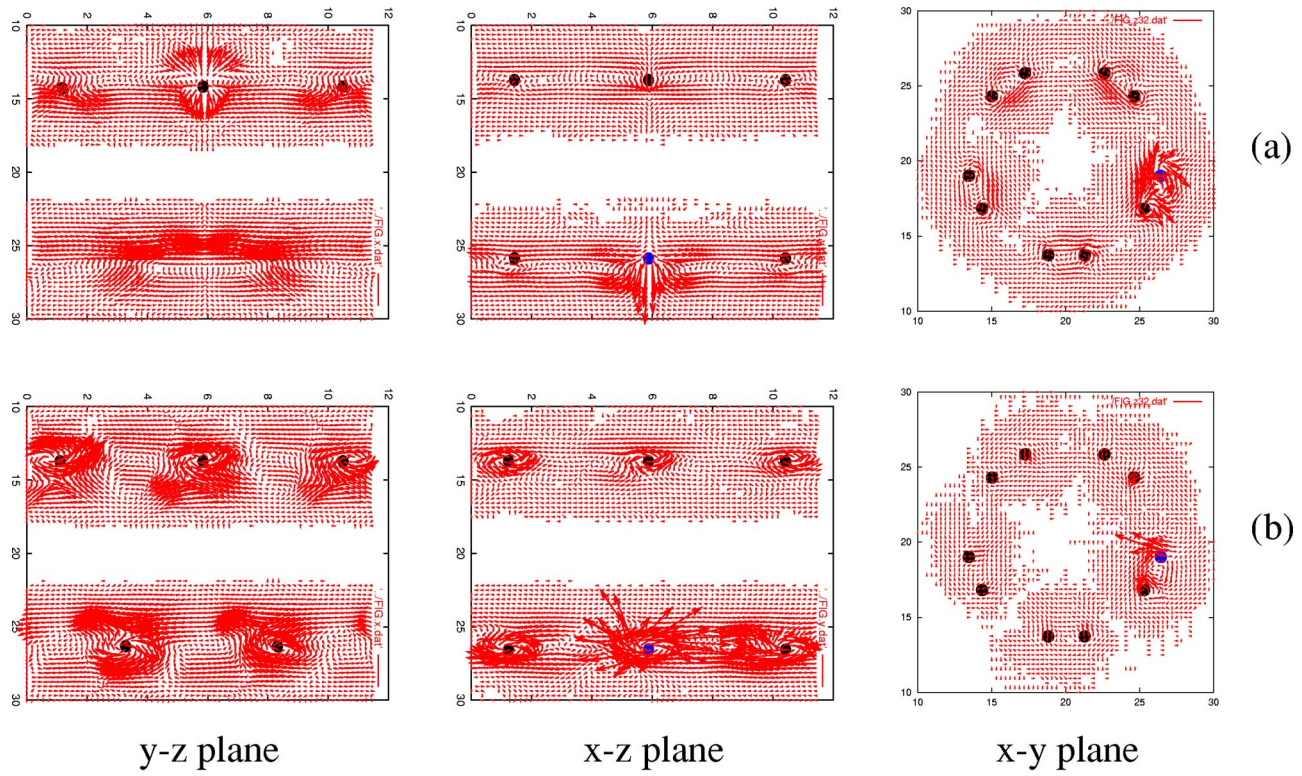

FIG. 4. (Color online) Distribution of the current density in the nitrogen-doped (5,5) nanotube. (a) The projections of current density at $V_b=0$, (b) at $V_b=0.8$ V.

atom [see Figs. 1(b), 1(c)]. In all the figures below, the x-y plane cuts through the impurity atom.

Figure 2 plots the current density of a perfect pristine (5,5) nanotube at $V_b=0$ [Fig. 2(a)] and $V_b=0.8$ V [Fig. 2(b)]. When bias is zero, the total current is zero but the current density is nonzero as shown in Fig. 2(a). More interesting is the result at a finite bias which drive a nonzero total current and breaks the left-right mirror symmetry of the tube. As shown in Fig. 2(b), there is a ''vortex'' around each carbon atom. This is not strange because there should be loop currents due to central potential of the atomic core. There is also a clear difference in the vortex shape for $V_b=0$ and 0.8 V. Figure 2(b) clearly shows a global flow of electric current along the nanotube due to the propagating scattering states under the finite bias.

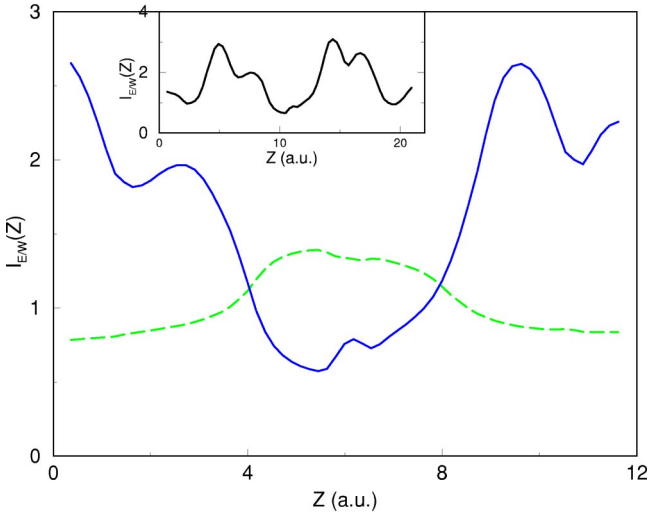

FIG. 5. (Color online) The ratio of the $I_{E/W}(Z)$ along the single B- and N-doped (5,5) nanotubes. Solid line is for the N-doped carbon nanotube and dashed line is for the B-doped carbon nanotube. Inset: the ratio for a longer N-doped (5,5) tube. Bias voltage $V_b=0.8$ V.

Figure 3 shows the current density of the boron doped (5,5) nanotube at $V_b=0$ [Fig. 3(a)] and $V_b=0.8$ V [Fig. 3(b)]. The substitutional impurity breaks the rotational symmetry of the original pristine nanotube. Accordingly, the distribution of current density in the boron doped nanotube is no longer perfectly symmetric. The boron substitutional impurity establishes quasibound defect states in continuum near the first lower subband of the nanotube device: this is analogous to acceptor levels of doped semiconductors as discussed in Ref. 30. Most striking, however, is the clear redistribution of current density. As shown in Fig. 3(b), current density in the x-z plane is markedly different from that of the pristine nanotube [Fig. 2(b)]: the boron impurity apparently ''repels'' current density, i.e., the presence of boron redistributes current density so that the side [see Fig. 1(d)] of the tube without B draws more current density. Note that since current density is a local quantity, its redistribution is not a constant along the tube.

Figure 4 shows the current density of nitrogen doped (5,5) nanotube at $V_b=0$ [Fig. 4(a)] and $V_b=0.8$ V [Fig. 4(b)]. Similarly, a nitrogen substitutional impurity also breaks the symmetry of the original bare (5,5) nanotube. The distribu-

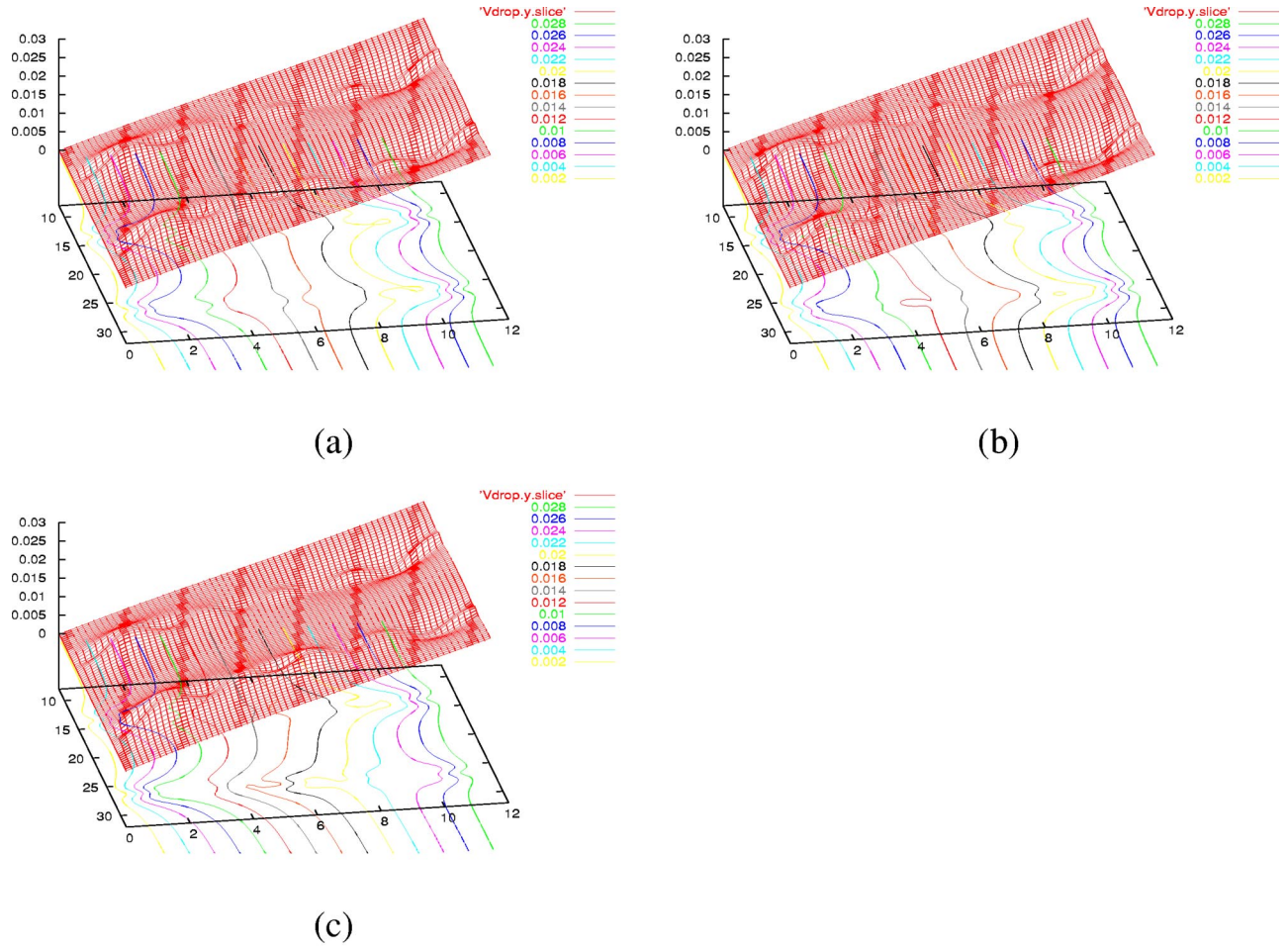

FIG. 6. (Color online) Potential drop at $V_b = 0.8$ V (0.03 a.u.) in the x-z plane along the pristine and B- and N-doped carbon nanotubes. (a) Pristine (5,5) carbon nanotube. (b) B-doped (5,5) nanotube. (c) N-doped (5,5) nanotube.

tion of current density in the nitrogen doped nanotube is no longer perfectly symmetric. In this case, the nitrogen impurity establishes quasibound defect states near the first upper subband of the device, analogous to donor levels of semiconductors.[30] Since the N impurity is more electronegative than carbon, it ''attracts'' current density to the side of the tube where it is located. Exactly opposite to the B-doped tube, for N-doped tubes the current density is mostly larger in the side of the nanotube where N resides [see Fig. 1(e)]. Again, the amount of redistribution varies along the tube axis.

As a rough estimate of the current density redistribution due to impurity doping, we calculate a total local current on the east/west (E/W) side of the ring [see Figs. 1(d), 1(e)] $I_{E/W}(Z) \equiv \int_C d\mathbf{s} J_z(Z)$ where Z is the position along the tube, $J_z(Z)$ is the current density along the tube at position Z, and the integral is on the perimeter C which is the east/west half circle in Figs. 1(d), 1(e). We present the ratio of the $I_{E/W}(Z)$ along the B- and N-doped carbon nanotubes in Fig. 5. Although quantity $I_{E/W}(Z)$ does not give a complete picture of the current flow, it gives a simple measure of the current density redistribution. Dividing the tube this way, the impurity is on the east side of the carbon ring. We found that the ratio $I_E/I_W < 1$ for the B-doped tube while it is > 1 for the N-doped tube when Z is about one or more bond length away from the impurity. However, in the very close vicinity of B, the ratio $I_E/I_W > 1$, and in the very close vicinity of N the ratio $I_E/I_W < 1$. The value of this ratio varies more along the N-doped tube than that along the B-doped tube, indicating that N impurity is more efficient in redistributing the current density than B in carbon nanotubes. Although we expect this ratio to reach unity very far away from the impurity, as shown in the inset of Fig. 5 for a longer tube doped with N, it is clear that the doped atom acts to redistribute current density near the impurity. Importantly, because current must flow continuously through the tube, the fact that I_E/I_W is not a constant along the tube near the impurity, suggests that there appears a chiral current which brings the current density from one side to the other side of our tube division.

Finally, Fig. 6 plots the potential drop at $V_b = 0.8$ V in the x-z plane along the pristine and B- and N-doped carbon nanotubes. Just as what happens to current density, the potential drop (Hartree potential in the DFT analysis) is also affected by the dopant atoms. In particular, the Hartree potential near the impurities become rather different than that near the carbon atom of the pristine tube, providing, in part, the local driving force that redistributes the current density and generating the chiral current component.

In summary, current density distribution is found to give a vivid picture on how current flows through the scattering region of a molecular electronic system. For the single B- and N-doped armchair (5,5) nanotube, a redistribution of current density occurs due to the impurity scattering and chiral current flow is deduced from the current density distribution near the scattering center. The more electronegative (compared with carbon) impurity of N acts to ''attract'' current density toward its neighborhood, while the less electronegative impurity of B ''repels'' current density (except at the immediate vicinity of the impurities). An interesting further investigation will be the current density distribution by periodically doping nanotubes with B and N impurities: this way the chiral component of the current density may be sustained along the nanotube for a long distance, making it acting as a nanoscale coil.[16]

We gratefully acknowledge financial support from the Natural Science and Engineering Research Council of Canada, le Fonds pour la Formation de Chercheurs et l'Aide à la Recherche de la Province du Québec, and NanoQuebec.

[1] For a review, see, for example, J.R. Heath and M.A. Ratner, Phys. Today **56**, 43 (2003).
[2] C. Joachim, J.K. Gimzewski, R.R. Schlittler, and C. Chavy, Phys. Rev. Lett. **74**, 2102 (1995); J.K. Gimzewski and C. Joachim, Science **283**, 1683 (1999).
[3] M.A. Reed, C. Zhou, C.J. Muller, T.P. Burgin, and J.M. Tour, Science **278**, 252 (1997).
[4] S.J. Tans, R.M. Verschueren, and C. Dekker, Nature (London) **393**, 49 (1998).
[5] S. Frank, P. Poncharal, Z.L. Wang, and W.A. de Heer, Science **280**, 1744 (1998).
[6] L.A. Bumm, J.J. Arnold, M.T. Cygan, T.D. Dunbar, T.P. Burgin, L. Jones II, D.L. Allara, J.M. Tour, and P.S. Weiss, Science **271**, 1705 (1996).
[7] R.P. Andres, J.O. Bielefeld, J.I. Henderson, D.B. Janes, V.R. Kolagunta, C.P. Kubiak, W.J. Mahoney, and R.G. Osifchin, Science **273**, 1690 (1997).
[8] J. Chen, M.A. Reed, A.M. Rawlett, and J.M. Tour, Science **286**, 1550 (1999).
[9] V. Mujica, M. Kemp, and M.A. Ratner, J. Chem. Phys. **101**, 6849 (1994).
[10] M.P. Samanta, W. Tian, S. Datta, J.I. Henderson, and C.P. Kubiak, Phys. Rev. B **53**, R7626 (1996).
[11] E.G. Emberly and G. Kirczenow, Phys. Rev. B **58**, 10 911 (1998).
[12] J. Taylor, H. Guo, and J. Wang, Phys. Rev. B **63**, 121104 (2001); **63**, 245407 (2001); J. Taylor, Ph.D. thesis, McGill University, 2000.
[13] M. Brandbyge, J.-L. Mozos, P. Ordejon, J. Taylor, and K. Stokbro, Phys. Rev. B **65**, 165401 (2002).
[14] Yongqiang Xue and S. Datta, Phys. Rev. Lett. **83**, 4844 (1999); Yongqiang Xue, S. Datta, and Mark A. Ratner, J. Chem. Phys. **115**, 4292 (2001).
[15] Brian Larade, Jeremy Taylor, Q.R. Zheng, Hatem Mehrez, Pawel Pomorski, and Hong Guo, Phys. Rev. B **64**, 195402 (2001).
[16] Yoshiyuki Miyamoto, Phys. Rev. B **54**, R11 149 (1996); Yoshiyuki Miyamoto, Steven G. Louie, and Marvin L. Cohen, Phys. Rev. Lett. **76**, 2121 (1996); Yoshiyuki Miyamoto, Angel Rubio, Marvin L. Cohen, and Steven G. Louie, Phys. Rev. B **50**, 4976 (1994).
[17] S. Nakanishi and M. Tsukada, Phys. Rev. Lett. **87**, 126801 (2001).
[18] P. Ordejón, E. Artacho, and J.M. Soler, Phys. Rev. B **53**, 10 441 (1996).
[19] D.R. Hamann, M. Schlüter, and C. Chiang, Phys. Rev. Lett. **43**, 1494 (1982).
[20] J.W. Mintmire, B.I. Dunlap, and C.T. White, Phys. Rev. Lett. **68**, 631 (1992).
[21] N. Hamada, S.I. Sawada, and A. Oshiyama, Phys. Rev. Lett. **68**, 1579 (1992).
[22] R. Saito, M. Fujita, G. Dresselhaus, and M.S. Dresselhaus, Appl. Phys. Lett. **60**, 2204 (1992).
[23] P.G. Collins, A. Zettl, H. Bando, A. Thess, and R. Smalley, Science **278**, 100 (1997).
[24] R.S. Lee, H.J. Kim, J.E. Fischer, A. Thess, and R.E. Smalley, Nature (London) **388**, 255 (1997).
[25] Z. Yao, H.W.Ch. Postma, L. Balents, and C. Dekker, Nature (London) **402**, 273 (1999).
[26] M. Bochrath, W. Liang, D. Bozovic, J.H. Hafner, C.H. Lieber, M. Tinkham, and H. Park, Science **291**, 283 (2001).
[27] L. Chico, V.H. Crespi, L.X. Benedict, S.G. Louie, and M.L. Cohen, Phys. Rev. Lett. **76**, 971 (1996).
[28] L. Chico, M.P. Lopez Sancho, and M.C. Muñoz, Phys. Rev. Lett. **81**, 1278 (1998).
[29] M.B. Nardelli, Phys. Rev. B **60**, 7828 (1999); M.B. Nardelli and J. Bernholc, *ibid.* **60**, R16 338 (1999).
[30] H.J. Choi, J. Ihm, S.G. Louie, and M.L. Cohen, Phys. Rev. Lett. **84**, 2917 (2000).
[31] Hai-Feng Song, Jia-Lin Zhu, and Jia-Jiong Xiong, Phys. Rev. B **65**, 085408 (2002).
[32] C.C. Kaun, B. Larade, H. Mehrez, J. Taylor, and H. Guo, Phys. Rev. B **65**, 205416 (2002).
[33] J.Y. Yi and J. Bernholc, Phys. Rev. B **47**, 1708 (1993).